Renewable Energy 44 (2012) 288–295

Contents lists available at SciVerse ScienceDirect

Renewable Energy

journal homepage: www.elsevier.com/locate/renene

Optimum load management strategy for wind/diesel/battery hybrid power systems

Juan M. Lujano-Rojas [a], Cláudio Monteiro [b,c], Rodolfo Dufo-López [a], José L. Bernal-Agustín [a,*]

[a] Department of Electrical Engineering, University of Zaragoza, 50018 Zaragoza, Spain
[b] FEUP, Fac. Engenharia Univ. Porto, Portugal
[c] INESC – Instituto de Engenharia de Sistemas e Computadores do Porto, Porto, Portugal

ARTICLE INFO

Article history:
Received 4 August 2011
Accepted 25 January 2012
Available online 8 February 2012

Keywords:
Load management strategy
Hybrid system
Controllable loads

ABSTRACT

This paper discusses a novel load management strategy for the optimal use of renewable energy in systems with wind turbines, a battery bank, and a diesel generator. Using predictions concerning wind speed and power, controllable loads are used to minimize the energy supplied by the diesel generator and battery bank, subject to constraints imposed by the user's behavior and duty cycle of the appliances. We analyzed a small hybrid power system in Zaragoza, Spain, and the results showed load management strategy allowed improvement in the wind power use by shifting controllable loads to wind power peaks, increasing the state of the charge in the battery bank, and reducing the diesel generator operating time, when compared to a case without load management.

1. Introduction

Management of hybrid power systems has two important components: a strategy for controlling energy sources and load management. In an important study, Barley and Winn [1] proposed the following general control strategies for systems with renewable energy sources, a diesel generator and a battery bank: the frugal dispatch strategy, the load following strategy, the state of charge (SOC) setpoint strategy, and the full power/minimum run time (FPMRT) strategy. In the frugal dispatch strategy, the intersection of the diesel energy cost curve with the battery wear cost line determines a critical load. If the net load (the difference between load and power from renewable sources) is higher than the critical load, the diesel generator is used; otherwise, the batteries are discharged. In the load following strategy, the diesel generator runs to match the instantaneous net load and never charges the batteries. In the state of charge (SOC) setpoint strategy, the diesel generator operates at full power until the SOC reaches the setpoint previously arranged. In the FPMRT strategy, the diesel generator operates for a predetermined length of time, charging the batteries with the excess energy, and then is disconnected. The authors used the predictive dispatch strategy as a benchmark for evaluating these strategies and found the actual use of the diesel generator and the battery bank depended on the critical load value in the future.

Ashari and Nayar [2] developed a control strategy for systems with renewable energy sources, diesel generators, and battery banks that uses power demand, battery bank voltage, and minimum power of a diesel generator to decide when to charge or discharge the battery bank and start or stop the diesel generator, i.e., the optimal strategy operation is searched, determining the load setpoint to start and stop the diesel generator and the SOC setpoint to charge the battery bank.

More recently, Dufo-López and Bernal-Agustín [3] analyzed combining the load following strategy and the state of charge set-point strategy proposed, by Barley and Winn [1], in photovoltaic systems combined with other sources of energy. They found that if the net load is lower than the critical load, the state of charge setpoint strategy should be applied; otherwise, the load following strategy should be applied.

Yamamoto et al. [4] proposed a predictive control method for systems with photovoltaic panels, diesel generators, and battery bank. Their strategy used the forecast of photovoltaic production and an hourly load profile to decide on the diesel generator output power. If the SOC of the battery bank was between 0.5 and 0.7, the diesel generator started and, when the SOC was higher than 0.7, the diesel generator stopped.

Concerning load management, Groumpos et al. [5] did the first work in stand-alone photovoltaic systems with a system located in the village of Schuchuli, Arizona (USA). In this system, four load

* Corresponding author. Tel.: +34 976761921; fax: +34 762226.
E-mail address: jlbernal@unizar.es (J.L. Bernal-Agustín).

0960-1481/$ – see front matter © 2012 Elsevier Ltd. All rights reserved.
doi:10.1016/j.renene.2012.01.097

priorities and four SOC setpoints (0.5, 0.4, 0.3 and 0.2) were established. For example, if the battery bank was discharging and the SOC setpoints values were sequentially reached, the loads were disconnected beginning with the lowest priority. Otherwise, if the battery bank was charging and the SOC setpoints values were sequentially reached, the loads were reconnected. The same authors, Groumps and Papegeorgiou, proposed in [6] an optimal load management technique for a stand-alone photovoltaic system based on three major categories of load classifications: an operational classification (DC and AC loads), a system classification (uncontrollable, controllable, and semi-controllable loads), and a priority classification (useful, essential, critical, and emergency loads). In this method, using the controllable load, the general load curve is manipulated to minimize the integral of the square of the net load over a 24-h period in order to reduce the required battery bank capacity and total life cycle costs.

Khouzam and Khouzam [7] developed a methodology for load management in stand-alone photovoltaic systems wherein the loads were classified into four general categories according to their priorities: convenient, essential, critical, and emergency; the priority of the battery bank was variable and dependent on the SOC. The optimal management was based on the maximization of an objective function that depended on the load priorities and was subject to the availability of an energy supply.

In another study, Moreno et al. [8] implemented a fuzzy controller to be applied to load management in stand-alone photovoltaic systems. The variable considered was supply expectancy predicted 1 h ahead in order to decide in real time whether to connect or disconnect the load according to its priority. Salah et al. [9] proposed a load management method for a domestic grid-connected photovoltaic system without batteries. In this approach, the photovoltaic generator was considered a complementary source of energy. This technique uses the fuzzy logic controller to decide in real time which appliance must be connected, the photovoltaic panel or the electric grid. The decision is made after considering photovoltaic and operating power, the priority of the appliances, and the maximum time the appliances are connected to the photovoltaic generator. This approach allows continuous energy savings. Ammar et al. [10] proposed a methodology for daily optimum management of a household photovoltaic system connected to the electrical grid without a battery bank. This approach uses predictions concerning photovoltaic generator production the next day to plan the connection times of appliances to the photovoltaic generator. The decision is made considering the duty cycle for each appliance. Similar criteria were used by Salah et al. in [9]. Finally, Thiaux et al. [11] analyzed the influence of the load profile shape on the energy cost of the life cycle of stand-alone photovoltaic systems. Their results showed the gross energy requirements are minimized when the load and photovoltaic production profiles are similar.

According to these papers, renewable power sources forecasting, control strategies for power sources, and load management are important in reducing the life cycle cost of a determined stand-alone hybrid power system. In this paper, we describe a novel load management strategy developed for the optimal use of renewable energy in systems with wind turbines, a battery bank, and a diesel generator.

This paper is organized as follows. In section 2, we provide a description of the wind/diesel/battery hybrid power system model. In section 3, we explain the prediction of the hourly average wind speed with the ARMA model. In section 4, we carefully detail the proposed load management strategy. We illustrate the load management strategy with a case study described in section 5, and we draw conclusions in the final section of the paper.

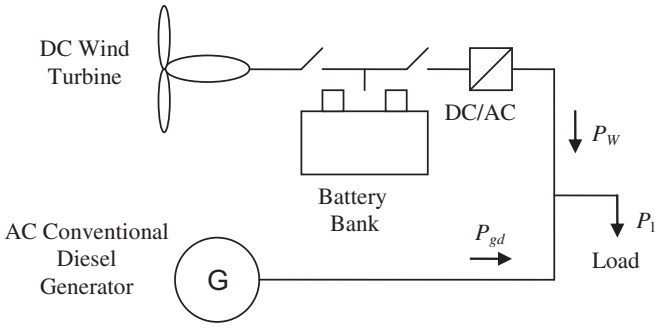

Fig. 1. AC coupled hybrid power system.

2. Wind/diesel/battery hybrid power system model

The system under study is the AC coupled hybrid power system [12] shown in Fig. 1. In this system, the small capacity wind turbine and the battery bank are coupled through a power inverter to an AC bus. The next sections describe the mathematical models for each component of the system.

2.1. Small capacity wind turbine model

The typical power curve of a small capacity wind turbine with horizontal axes is shown in Fig. 2; this curve can be obtained using data in discrete form frequently provided by the manufacturer. In this type of wind turbine, the start-up wind speed is between 3 and 4 m/s, and the rated power is reached for wind speeds between 14 and 15 m/s. When the wind speed is higher than 14 or 18 m/s, the power production falls to between 30 and 70% of the rated power [13].

2.2. Lead acid battery bank and charge controller model

Coppeti and Chenlo [14] proposed that a lead acid battery model is able to adequately represent the complex behavior of the charge and discharge processes in the battery [15]; however, their mathematical formulation was very complex because it needed to solve a nonlinear equations system for each hour of simulation. Therefore, for the purposes of this paper, we simplified this model, which is normalized with respect to the total ampere-hours that may be charged or discharged in 10 h at 25 °C (C_{10} capacity), and it considers the low current operation and temperature effects of the battery capacity. Equations (1) and (2) show the capacity equation [14].

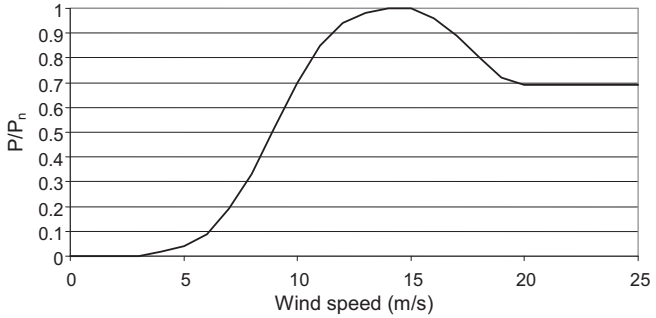

Fig. 2. Typical power curve of small wind turbine.

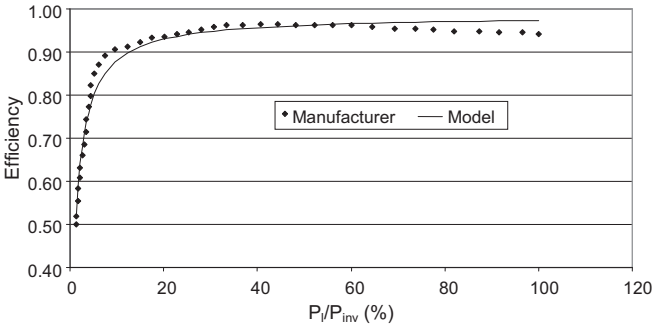

Fig. 3. Typical inverter efficiency curve.

$$C_T = 1.67C_{10}(1 + 0.005\Delta T_a) \tag{1}$$

$$C = \frac{C_T}{1 + 0.67\left(\frac{I}{I_{10}}\right)^{0.9}} \tag{2}$$

where $\Delta T_a = T_a - 25$ is the temperature variation from the reference of 25 °C, and T_a is the ambient temperature in °C, C_T is the maximum capacity of the battery (Ah), and C is the ampere-hours capacity at the charge or discharge constant current I (A).

During the charge process ($I > 0$), the coulombic efficiency is defined as the ratio of the number of coulombs that effectively have been stored in the battery to the number of coulombs supplied to the battery; in contrast, during the discharge process ($I < 0$), the coulombic efficiency is defined as the ratio of the number of coulombs that can be discharged from the battery to the number of coulombs initially stored in it. The coulombic efficiency (η_b) during the discharge and charge process is calculated using equation (3) [16].

$$\eta_b = \begin{cases} 1 - \exp\left[\left(\frac{20.73}{I/I_{10} + 0.55}\right)(SOC - 1)\right] & I > 0 \\ 1 & I < 0 \end{cases} \tag{3}$$

where I_{10} (A) is the charge or discharge current in 10 h at 25 °C. The state of charge (SOC) of the battery (value between 0 and 1) is calculated using equation (4).

$$SOC = \begin{cases} \frac{Q}{C}\eta_b & I > 0 \\ 1 - \frac{Q}{C}\eta_b & I < 0 \end{cases} \tag{4}$$

where $Q = |I|t_b$ (Ah) is the charge supplied by the battery (discharge) or to the battery (charge) during a particular time t_b (h). An important factor in the operation of the hybrid power system using lead acid batteries is the effect of voltage stability on energy capture. This is important because high charge currents produce a DC bus with high voltage, and the charge controller disconnects the wind turbine before the battery bank is completely charged [17], so it is necessary to consider the charge controller in the hybrid system model, although it is not considered in most of the models used to simulate and optimize this kind of system. Considering the joint effect of ambient temperature, coulombic efficiency, and charge controller operation allows a high degree of accuracy in the simulation of the system.

The battery voltage at which the charge controller disconnects the wind turbine is between 2.40 and 2.55 V per cell [18] and, during this process, the battery voltage per cell (V) may be approximated by equation (5) [14].

$$V = \left(2 + 0.16\frac{Q}{C}\right) + \frac{I}{C_{10}}\left(\frac{6}{1 + I^{0.6}} + \frac{0.48}{(1 - Q/C_T)^{1.2}} + 0.036\right) \times (1 - 0.025\Delta T_a) \tag{5}$$

For example, if the charge controller setpoint is 2.50 V per cell, the equation (5) allows one to estimate the Q value at which the

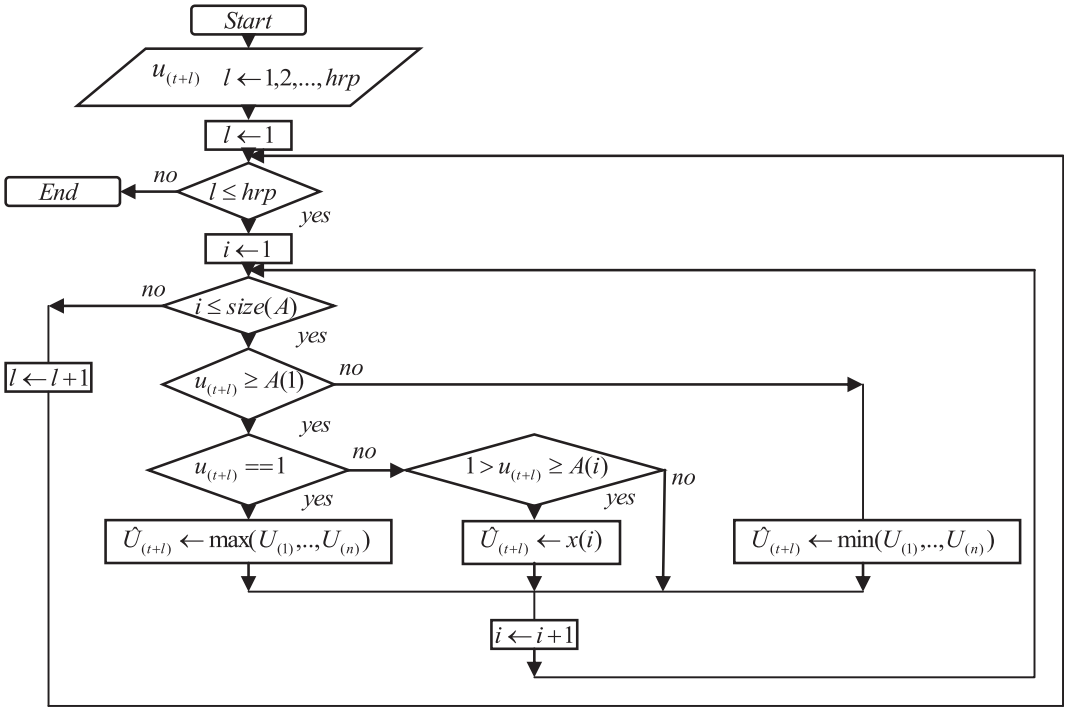

Fig. 4. Algorithm to calculate the inverse of the CDF in discrete form.

battery voltage is 2.50 V per cell and, therefore, the moment at which the charge controller disconnects the wind generator, (the state of charge of the battery bank limited at this value). During the discharge process, when the state of charge is equal to the minimum value specified by the battery manufacturer, the charge controller disconnects the load of the battery bank to prevent over-discharge.

2.3. Inverter model

The inverter is modeled by its efficiency (η_i) calculated by equation (6).

$$\eta_i = \frac{P_l}{k_0 P_{inv} + (1 + k_1) P_l} \tag{6}$$

where P_l is the load in the AC bus, P_{inv} is the rated power of the inverter, and k_0 and k_1 are parameters determined from the data supplied by the manufacturer. Fig. 3 shows the efficiency curve of a typical power inverter with $k_0 = 0.0119$ and $k_1 = 0.0155$. An important consideration is that the efficiency drops when the load is lower than 10% of the rated power.

2.4. Diesel generator model

The fuel consumption of the diesel generator, $F_l\,(1)$, is calculated using equation (7).

$$F_l = k_2 P_{gdn} + k_3 P_{gd} \tag{7}$$

where P_{gdn} (kW) is the rated power of the diesel generator, P_{gd} (kW) is the power generated at the time of interest, and k_2 and k_3 are parameters determined from the data supplied by the manufacturer (the typical values for these parameters are $k_2 = 0.085$ l/kWh and $k_3 = 0.246$ l/kWh [19]).

3. Hourly wind speed prediction method

Hourly average wind speed forecasting using only the time series is typically made with an autoregressive moving average (ARMA) model. The methodology to fit the ARMA model was presented in [20] and will be briefly explained in the next sections.

3.1. ARMA model

The autoregressive moving average (ARMA) model is:

$$\hat{W}_{(t)} = \phi_1 \hat{W}_{(t-1)} + \ldots + \phi_p \hat{W}_{(t-p)} + \varepsilon_{(t)} - \theta_1 \varepsilon_{(t-1)} - \ldots - \theta_q \varepsilon_{(t-q)} \tag{8}$$

where $\hat{W}_{(t)}$ is the transformed and standardized wind speed time series, $\phi_1,\ldots,\phi_p$ are the autoregressive parameters, $\theta_1,\ldots,\theta_q$ are the moving average parameters, and $\varepsilon_{(t)}$, $\varepsilon_{(t-1)},\ldots,\varepsilon_{(t-q)}$ are random variables with a mean of zero and a standard deviation of σ. Calculation of autoregressive and moving average parameters requires transformation, standardization, estimation, and diagnostic checking processes.

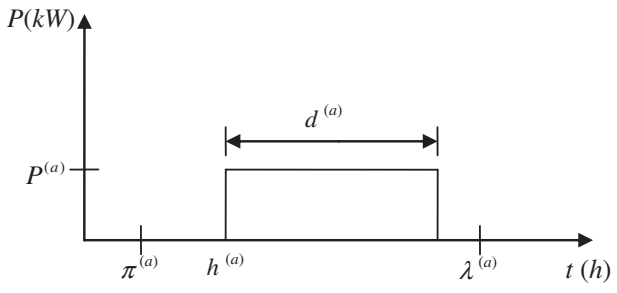

Fig. 5. Idealized load profile of appliance *a*.

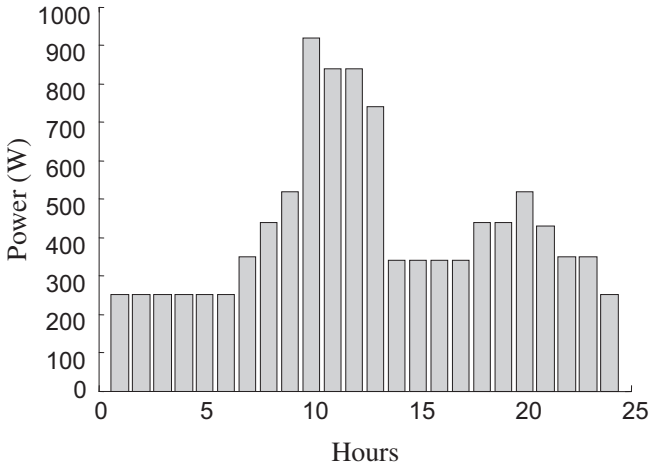

Fig. 6. Typical load profile for case study.

3.1.1. Transformation and standardization

The probability density function (PDF) of a wind speed time series frequently is a Weibull distribution with a determined shape factor *k*, so the first step in the wind speed time series analysis consists of transforming the time series to another one that has a Gaussian PDF. This transformation is shown in equation (9) [21]:

$$U_{T(t)} = U_{(t)}^{m} \text{ with } t = 1,\ldots,n \tag{9}$$

where $U_{(t)}$ is the wind speed time series under study, $U_{T(t)}$ is the time series with a Gaussian PDF, n is the total number of observations, and m is the power transformation between $k/3.60$ and $k/3.26$, according to Dubey (1967) [22]. The selected value of m is that for which the coefficient of skewness (SK) is closest to zero. The coefficient of skewness is calculated by equation (10) [23].

$$SK = \frac{Q_3 + Q_1 - 2Q_2}{Q_3 - Q_1} \tag{10}$$

where $Q_1 = A^{-1}(0.25)$, $Q_2 = A^{-1}(0.5)$, and $Q_3 = A^{-1}(0.75)$ are the first, second, and third quartiles, respectively. $A^{-1}(.)$ is the inverse of

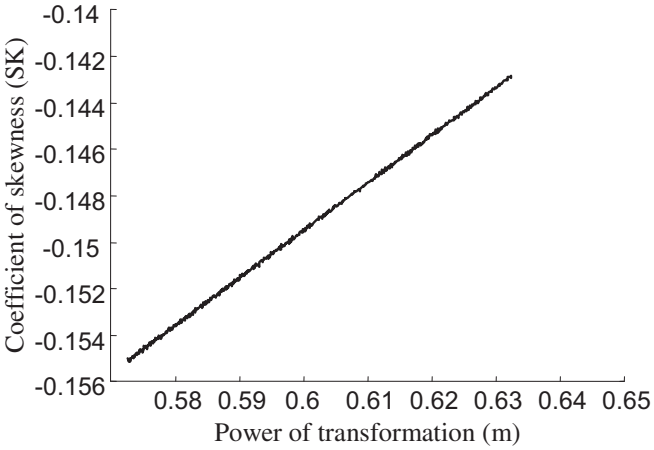

Fig. 7. Coefficient of skewness vs. power of transformation.

Table 1
Characteristics of ARMA model.

(p,q)	L-p-q	$\chi^2(\alpha = 0.05)$	S	m	ϕ_1	ϕ_2	k	Criterio	Δx
(2,0)	73	93.9453	86.2816	0.6323	0.7225	0.2178	2.0615	BIC	0.0001

the Cumulative Distribution Function (CDF) calculated using the algorithm shown in Fig. 4 (Section 3.1.4). In order for the time series $U_{T(t)}$ to be stationary, it is necessary to subtract the hourly average and divide by the hourly standard deviations. If $\mu_h(h)$ and $\sigma_h(h)$ with $h = 1,2,\ldots,24$ are the hourly average and standard deviation of transformed wind speed series, respectively, it is assumed that these functions are periodic: $\mu_h(h = 25) = \mu_h(h = 1)$ and $\sigma_h(h = 25) = \sigma_h(h = 1)$ [21]. The transformed and standardized series ($W_{(t)}$) is:

$$W_{(t)} = \frac{U_{T(t)} - \mu_{h(t)}}{\sigma_{h(t)}} \tag{11}$$

3.1.2. Estimation

The order of the ARMA (*p*,*q*) model can be estimated using the plots of autocorrelation function (ACF) and partial autocorrelation function (PACF). For example, in a pure autoregressive process of order *p*, the ACF tails off, while PACF has a cut-off value after lag *p* [24]. Others' approaches use the Bayesian Information Criterion (BIC) [25] and Akaike Information Criterion (AIC) [26]. The *p* and *q* values are selected, minimizing the respective criterion BIC or AIC of equations (12) and (13).

$$BIC(p,q) = n\log\left(\sigma^2_{(p,q)}\right) + (p+q)\log(n) \tag{12}$$

$$AIC(p,q) = n\log\left(\sigma^2_{(p,q)}\right) + 2(p+q) \tag{13}$$

$$\sigma^2_{(p,q)} = \frac{\sum_{t=1}^{n}\left(W_{(t)} - \hat{W}_{(t)}\right)^2}{n-(p+q)} \tag{14}$$

where $\sigma^2_{(p,q)}$ is the variance of the residual and $\hat{W}_{(t)}$ is the value calculated by the ARMA model. The autoregressive and moving average parameters are calculated by minimizing the quadratic prediction error criterion [27].

3.1.3. Diagnostic checking

The verification and statistical checking of the ARMA model fitted in the previous steps is carried out using the test of randomness proposed by Ljung and Box [28], which is determined according to the statistics of equation (15).

$$S = n(n+2)\sum_{\beta=1}^{L}\frac{r_\beta^2}{(n-\beta)} \tag{15}$$

where *L* is a number of lags considered and r_β is the correlation coefficient of the residuals corresponding to lag β. Under the null hypothesis of randomness, the asymptotic distribution of *S* is chi-square with *L-p-q* degrees of freedom $\chi^2(L\text{-}p\text{-}q)$. The null hypothesis of randomness, considering a determined level of significance α, is rejected if the statistics *S* is higher than $\chi^2_\alpha(L\text{-}p\text{-}q)$.

3.1.4. Forecasting of hourly average wind speed with the ARMA model

The first step in wind speed forecasting is to evaluate equations (16) and (17).

$$\hat{W}_{(t+l)} = \phi_1 W_{(t-1+l)} + \ldots + \phi_p W_{(t-p+l)} + \varepsilon_{(t+l)} - \theta_1\varepsilon_{(t-1+l)} - \ldots - \theta_q\varepsilon_{(t-q+l)} \tag{16}$$

$$\hat{U}_{T(t+l)} = \mu_{h(t+l)} + \sigma_{h(t+l)}\hat{W}_{(t+l)} \tag{17}$$

where $l = 1,\ldots,hrp$ and *hrp* are the hours ahead of prediction. In order to undo the transformation process, it is necessary to apply the probability transformation in the discrete form. Using this transformation, the PDF of hourly wind speed predicted will be the PDF of the original wind speed time series. This probability transformation is based on equation (18) below [29], and the forecasting values $\hat{U}_{(t+l)}$ are calculated using the next following equation (19).

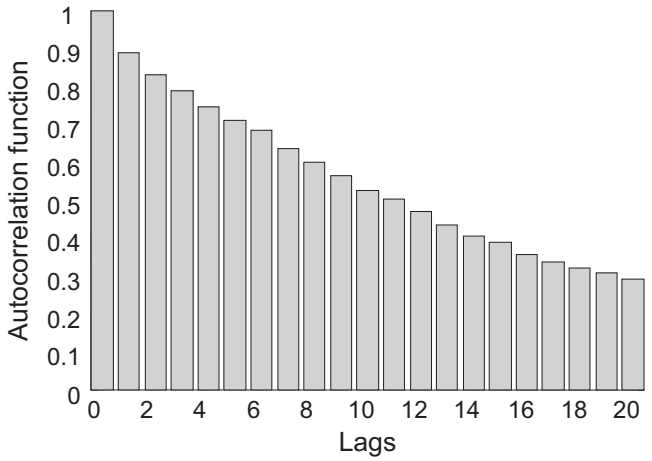

Fig. 8. Autocorrelation function.

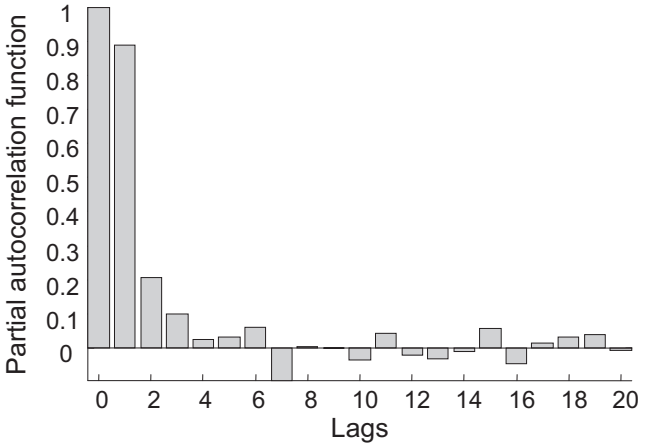

Fig. 9. Partial autocorrelation function.

Table 2
Forecasting errors 24 h ahead.

Index of error	Error
MBE (m/s)	−0.2600
RMSE (m/s)	2.5638
MABE (m/s)	1.9954
R	0.4635

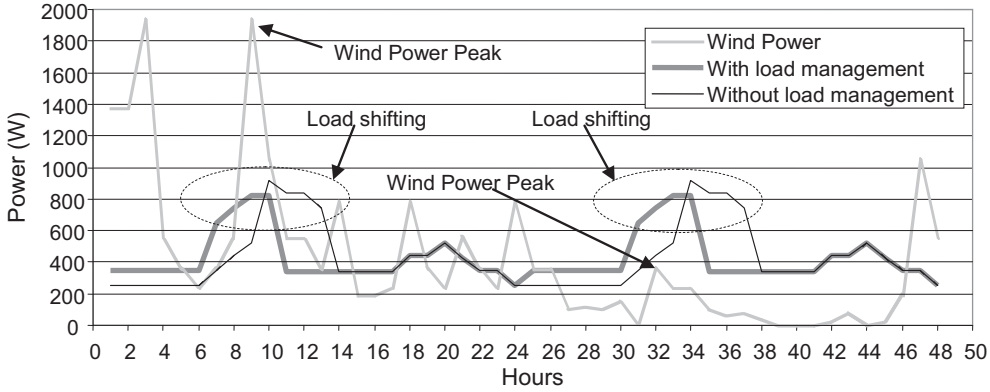

Fig. 10. Wind power and load profiles for 5th and 6th of August 2005.

$$A\left(\hat{U}_{(t+l)}\right) = u_{(t+l)} = \hat{A}_T\left(\hat{U}_{T(t+l)}\right) \tag{18}$$

$$\hat{U}_{(t+l)} = A^{-1}\left(\hat{A}_T\left(\hat{U}_{T(t+l)}\right)\right) \tag{19}$$

where A is the CDF in a discrete form of the original wind speed time series $U_{(t)}$, $\hat{A}_T$ is the CDF of the Gaussian distribution with a mean and standard deviation equal to the transformed time series $U_{T(t)}$, and $u_{(t+l)}$ is a random variable uniformly distributed and calculated using equation (18). To calculate the $\hat{U}_{(t+l)} = A^{-1}(u_{(t+l)})$ value, it is necessary to build the vector x, whose elements are zero *ceil* (max($U_{(t)}$)) with $t = 1,2,\ldots,n$ in step Δx. The next step is to build the vector A, whose elements are the cumulative probabilities of each element of vector x. The predicted value of the hourly wind speed $\hat{U}_{(t+l)}$ is calculated using the algorithm in Fig. 4. In this figure, the function *size* (A) calculates the number of rows of vector A.

4. Predictive load management

The load demand of the hybrid power system of Fig. 1 may be managed to reduce the daily fuel consumption; this is done using controllable loads when wind speed will be high.

If a is the number of controllable loads, Fig. 5 shows its idealized load profile.

Where $\pi^{(a)}$ is the earliest hour at which appliance a must start its operation, $\lambda^{(a)}$ is the latest hour at which appliance a must end its operation, $d^{(a)}$ is the duration of the operation of appliance a, $h^{(a)}$ is the possible hour at which appliance a will start its operation, $P^{(a)}$ is the power required by appliance a, and T (h) is the period of management. The load management consists of making forecasts of the hourly average wind speed and wind power in $T = 24$ h ahead. Using these predictions, it is possible to set the hour at which the appliance a will start its operation for minimizing the energy supplied by the controllable power sources (diesel generator and battery bank), using the load following strategy. In this paper, the optimization is made by testing all possible combinations. The mathematical formula of this problem is:

$$\min f = \sum_{l=1}^{l=T} k_4 \Psi(LHV)\left(k_2 P_{gdn} + k_3 P_{gd}(l)\right) + k_5 V_{DC}(\Delta \mathrm{SOC})C \tag{20}$$

It is subject to the following constraints:

$$P_l(l) = P_W(l) + P_{gd}(l) \text{ with } l = 1,2,\ldots,T \tag{21}$$

$$h^{(a)} \geq \pi^{(a)} \text{ with } a = 1,2,.. \tag{22}$$

$$h^{(a)} + d^{(a)} \leq \lambda^{(a)} \tag{23}$$

where f (kWh) is the entire amount of energy supplied by the diesel generator and the battery bank during the period of management T, Ψ is the density of fuel (0.82 kg/l), LHV is the lower heating value of fuel (43.2 MJ/kg), V_{DC} is the nominal voltage of the DC bus, ΔSOC is

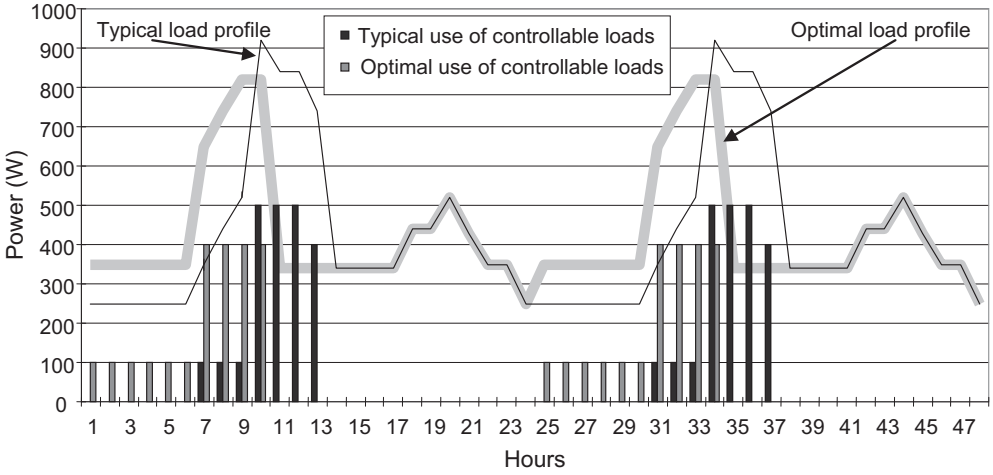

Fig. 11. Controllable loads management for 5th and 6th of August 2005.

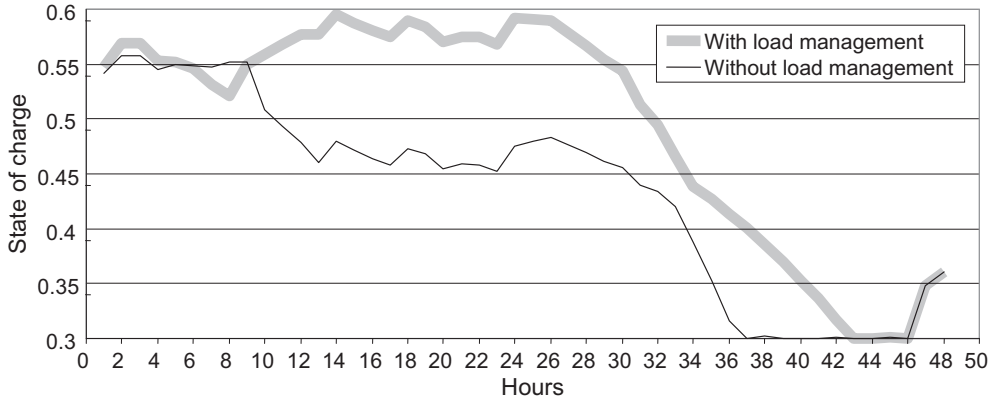

Fig. 12. State of charge for 5th and 6th of August 2005.

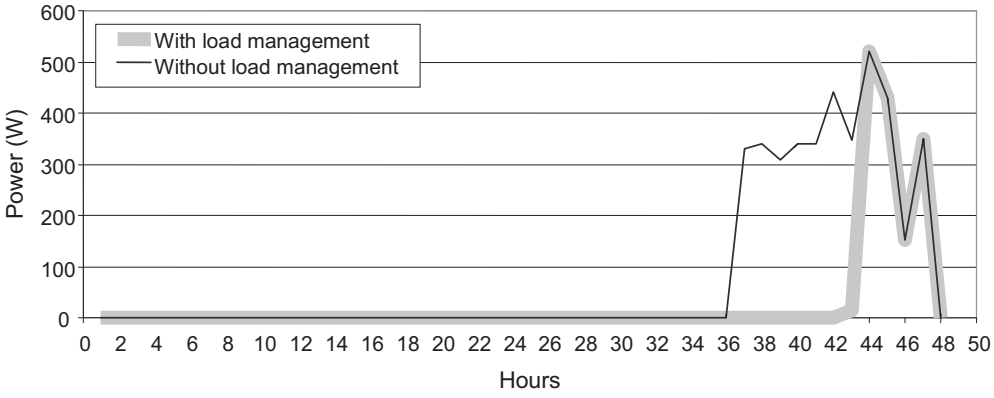

Fig. 13. Diesel generator output power for 5th and 6th of August 2005.

the decrement of the state of the charge when the battery bank is discharged, and k_4 and k_5 are conversion factors ($k_4 = 2.7 \times 10^{-4}$ and $k_5 = 10^{-3}$). $P_l(l)$, $P_W(l)$, and $P_{gd}(l)$ are the power levels demanded by the load, the total power produced by the wind turbine and battery bank, and the power produced by the diesel generator, respectively, during hour l, expressed in kW. The variables $\pi^{(a)}$ and $\lambda^{(a)}$ are imposed by the user of the hybrid power system and $d^{(a)}$ is imposed by the duty cycle of appliance a.

5. Case study

The load management strategy is illustrated using the system shown in Fig. 1 with a typical power demand (P_l) shown in Fig. 6. The system has two controllable loads ($a = 1,2$) that frequently operate for between 7 and 18 h ($\pi^{(1)} = 7$ and $\lambda^{(1)} = 18$) and between 1 and 24 h ($\pi^{(2)} = 1$ and $\lambda^{(2)} = 24$), consuming 400 W during 4 h and 100 W during 6 h, respectively. The system has a small wind turbine of 3500 W, a diesel generator of 1 kW, an inverter of 1 kW, and a battery bank of 6 cells in serial, 2 V, and $C_{10} = 1000$ Ah. The data collected in July 2005 in Zaragoza was used to fit the ARMA model. The forecasting error was calculated using data collected in August 2005. Fig. 7 shows the coefficient of skewness for different values of the power transformation shown in section 3.1.1 and the selected value shown in Table 1. Figs. 8 and 9 show the autocorrelation functions and partial autocorrelation function of transformed and standardized wind speed time series in July. The forecasting errors index containing the mean bias error (MBE), root mean square error (RMSE), mean absolute bias error (MABE), and correlation coefficient (R) are shown in Table 2. The load management strategy proposed in this paper and load following strategy, using the typical load profile of the Fig. 6, were applied to control the system of the study case simulated in August 2005 in Zaragoza without considering the temperature effects. The simulation of August 5th and 6th is shown in Figs. 10–13 Figs. 10 and 11 show the load is shifting to the wind power peak, i.e., the load profile with load management minimizing the energy supplied by the diesel generator and the battery bank (equation (20), with constraints (21), (22) and (23)). Fig. 12 shows the effect of the load shifting in the state of charge, which allows improving wind power use, increasing the state of the battery bank charge, and reducing the number of hours the diesel generator is operated, according to Fig. 13. For this case study, compared with the case without load management, the energy supplied by the diesel generator is reduced 4.6%.

6. Conclusions

In this paper we propose an optimum load management technique for hybrid systems with wind power, a battery bank, and a diesel generator. A controllable loads strategy is used to minimize the energy supplied by the diesel generator and battery bank, subject to constraints imposed by the user's behavior and duty cycle of the appliances. The results show that the load management strategy allows improvement of wind power usage by shifting controllable loads to wind power peaks (Figs. 10 and 11), increasing the state of charge in the battery bank (Fig. 12), and reducing the diesel generator operation time (Fig. 13), compared to the case without load management. However, due to a forecasting error in the hourly wind speed, in some cases the load shifting of the controllable loads may not be optimal.

Acknowledgments

This work was supported by the "Ministerio de Ciencia e Innovación" of the Spanish Government under Project ENE2009-14582-C02-01.

References

[1] Barley CD, Winn B. Optimal dispatch strategy in remote hybrid power systems. Solar Energy 1996;58(4–6):165–79.
[2] Ashari M, Nayar CV. An optimum dispatch strategy using set points for a photovoltaic (PV)–diesel–battery hybrid power system. Solar Energy 1999; 66(1):1–9.
[3] Dufo-López R, Bernal-Agustín JL. Design and control strategies of PV–diesel systems using genetic algorithms. Solar Energy 2005;79(1):33–46.
[4] Yamamoto S, Park JS, Takata M, Sasaki K, Hashimoto T. Basic study on the prediction of solar irradiation and its application to photovoltaic-diesel hybrid generation system. Solar Energy Materials and Solar Cells 2003;75(3–4): 577–84.
[5] Groumpos PP, Cull RC, Ratajczak AF. An overview of control aspects of a village stand-alone photovoltaic power system. IEEE Transaction on Power Apparatus and Systems 1984;103(10):2845–53. PAS.
[6] Groumps PP, Papegeorgiou G. An optimum load management strategy for stand-alone photovoltaic power systems. Solar Energy 1991;46(2):121–8.
[7] Khouzam K, Khouzam L. Load prioritization and shedding in photovoltaic power systems. Solar Cells 1991;31(6):505–11.
[8] Moreno A, Julve J, Silvestre S, Castañer L. A fuzzy logic controller for stand alone PV systems. IEEE Photovoltaic; 2000:1618–21. Specialists Conference.
[9] Salah CB, Chaabene M, Ammar MB. Multi-criteria fuzzy algorithm for energy management of a domestic photovoltaic panel. Renewable Energy 2008; 33(5):993–1001.
[10] Ammar MB, Chaabene M, Elhajjaji A. Daily energy planning of a household photovoltaic panel. Applied Energy 2010;87(7):2340–51.
[11] Thiaux Y, Seigneurbieux J, Multon B, Ahmed HB. Load profile impact on the gross energy requirement of stand-alone photovoltaic systems. Renewable Energy 2010;35(3):602–13.
[12] Moutawakkil K, Elster S. Re hybrid systems: coupling of renewable energy sources on the AC and DC side of the inverter. Refocus 2006;7(5):46–8.
[13] Jimenez AC, Olson K. Energía renovable para centros de salud rurales. USA: National Renewable Energy Laboratory, http://www.nrel.gov/docs/fy99osti/26224.pdf; 1998. Available from:.
[14] Copetti JB, Chenlo F. Lead/acid batteries for photovoltaic applications. Test results and modeling. Journal of Power Sources 1994;47(1–2):109–18.
[15] Achaibou N, Haddadi M, Malek A. Lead acid batteries simulation including experimental validation. Journal of Power Sources 2008;185(2):1484–91.
[16] Copetti JB, Lorenzo E, Chenlo F. A general battery model for PV system simulation. Progress in Photovoltaics 1993;1(4):283–92.
[17] Corbus D, Newcomb C, Baring-Gould EI, Friedly S. Battery voltage effects on small wind turbine energy capture. USA: National Renewable Energy Laboratory. Available at: http://www.nrel.gov/docs/fy02osti/32511.pdf; 2002.
[18] IEEE Standards Coordinating Committee 21. IEEE guide for selection, charging, test, and evaluation of lead-acid batteries used in stand-alone photovoltaic systems. IEEE Std; 2003. 1361.
[19] Skarstein O, Ulhen K. Design considerations with respect to long-term diesel saving in wind/diesel plants. Wind Engineering 1989;13(2):72–87.
[20] Lujano-Rojas JM, Bernal-Agustín JL, Dufo-López R, Domínguez-Navarro JA. Forecast of hourly average wind speed using ARMA model with discrete probability transformation. Lecture Notes in Electrical Engineering 98. Springer-Verlag; 2011. p. 1003–10.
[21] Brown BG, Katz RW, Murphy AH. Time series models to simulate and forecast wind speed and wind power. Journal of Climate and Applied Meteorology 1984;23(8):1184–95.
[22] Dubey SD. Normal and Weibull distributions. Naval Research Logistics Quarterly 1967;14(1):69–79.
[23] Kim TH, White H. On more robust estimation of skewness and kurtosis. Finance Research Letters 2004;1(1):56–73.
[24] Box JEP, Jenkins GM. Time series analysis: forecasting and control. Upper Saddle River, NJ: Prentice-Hall, Inc; 1976.
[25] Schwarz G. Estimating the dimension of a model. The Annals of Statistics 1978;6(2):461–4.
[26] Akaike H. A new look at the statistical model identification. IEEE Transactions on Automatic Control 1974;19(6):716–23.
[27] Ljung L. System identification. Theory for the user. PTR Prentice Hall; 1999. Information and System Sciences Series.
[28] Ljung GM, Box GEP. On a measure of lack of fit in time series models. Biometrika 1978;65(2):297–303.
[29] Rosenblatt M. Remarks on a multivariate transformation. Annals of Mathematical Statistics 1952;23(3):470–2.